The influence of paleoclimatic events on the functioning of an alpine thermal system (France): the contribution of hydrodynamic–thermal modeling

Stéphanie Gallino · Jean-Yves Josnin · Marc Dzikowski · Fabien Cornaton · Dominique Gasquet

Abstract Numerical models of the Aix-les-Bains thermal aquifer (France) were used to investigate the influence of Quaternary paleoclimatic events on the current thermal state of the groundwater. Initial numerical tests were successful in that present-day fluid flows (heads and flow rates) and the resulting velocities were compatible with residence time data. Water flowing through an aquifer cools the rock mass; therefore, the rate of water flow governs the outlets temperature. For the Aix-les-Bains aquifer, applying present-day flow rates to the entire history of the aquifer leads to much more substantial cooling of the rock mass than is indicated by the outlets temperature (i.e. present-day flow rates are 10 times too high). This suggests that the aquifer may have gone through alternating functioning phases, during which the rock mass cooled, and blocked phases, during which the aquifer reheated. Other results indicate that the main parameters affecting thermal behavior during a functioning phase are the total inflow volume, rather than individual inflow rates, and the initial heat field. As phenomena linked to glaciation can lead to the blocking of infiltration zones and aquifer outlets, the findings suggest that the hypothesis of intermittent aquifer functioning related to glaciations is compatible with the current thermal field.

Keywords Paleoclimatic events · Numerical modeling · Thermal conditions · Quaternary glaciations · France

S. Gallino (✉) · J.-Y. Josnin · M. Dzikowski · D. Gasquet
Laboratoire EDYTEM,
Université de Savoie, CNRS,
Campus Scientifique Bâtiment «Pôle Montagne», 73376,
Le Bourget Du Lac cedex, France
e-mail: Stephanie.gallino@univ-savoie.fr
Tel.: +33-4-79759453
Fax: +33-4-79758171

F. Cornaton
CHYN UNINE,
Rue Emile Argand 11, CP158 2009, Neuchatel, Switzerland

Introduction

Early hydrodynamic and thermal models were designed to provide analytical solutions to problems such as the disruption of temperature profiles at depth caused by circulating water (Bredehoeft and Papadopulos 1965). Mansure and Relter (1979) used Bredehoeft and Papadopulos's one-dimensional (1D) analytical solution to demonstrate that water flows that are not vertical and parallel to the heat flux substantially reduce the geothermal gradient and the heat flux. This 1D analytical solution was later developed into a 2D solution by Ziagos and Blackwell (1986) and by Lu and Ge (1996), who showed that when horizontal fluid and heat flows are comparable they can affect the vertical temperature gradient.

Hydrodynamic–thermal modeling has been used in a variety of studies such as:

1. *Preliminary studies for tunnel excavations* (Maréchal and Perrochet 1999, 2001). Hydrothermal simulation models based on studies conducted during the excavation of the Simplon (Switzerland—Italy) and Mont-Blanc (France-Italy) tunnels have been used to predict inflows and temperatures of water during tunneling operations. Strong negative temperature anomalies encountered during drilling may indicate areas in which cold water from the surface is circulating.
2. *Oil and gas exploration and production*. Hydrodynamic–thermal modeling of sedimentary basins has been used to characterize fluid flows (Bredehoeft and Papadopulos 1965; Woodbury and Smith 1988; Wang and Beck 1988), petroleum generation and migration (Ungerer et al. 1990; Person et al. 1995) and rock deformation (Ge and Garven 1992).
3. *Management of thermo-mineral aquifers (spas and bottled waters)*. Hydrodynamic–thermal methods have been used to model the Quézac and Plancoët (Durand 2005), and Dax (Le Fanic 2005) thermo-mineral aquifers in France. However, these models focused on

outlet areas and were designed as management tools for planning future drilling operations.

As the buffering effect of thermo-mineral aquifers results in long residence times for groundwaters, models of aquifer systems must take into account paleoclimatic events. For example, the Pleistocene glaciations may have influenced thermal systems in present-day temperate regions. Most recent studies of the effects of glaciations have investigated continental-scale phenomena, glacier tongues or valley glaciers.

1. *Continental-scale studies*. Some hydrodynamic–thermal modeling conducted on a continental scale in North America has shown that infiltration volumes may have been greater during glacial periods than during interglacial periods (Bense and Person 2008; Lemieux et al. 2008a). These higher infiltration volumes are the consequences of the spatial distribution of permafrost and of melting under ice sheets (Person et al. 2007). Permafrost, which divides hydraulic conductivities by six, is present only along the margins of ice sheets. Temperatures under ice sheets are slightly higher than temperatures along ice-sheet margins because of the blanket effect and because of the pressure exerted by the ice sheet. These two phenomena can raise temperatures sufficiently for melting to occur, thereby allowing infiltration and the development of eskers.

   Lemieux et al. (2008a) reported infiltration rates ranging from $1.3{\cdot}10^{-3}$ to 12 mm/year. Boulton et al. (1996) obtained similar results in Europe (Scandinavian shield), with infiltration rates ranging between 0 and 15 mm/year.

   On the other hand, Walvoord and Striegl (2007) show that the increase of flow rates of the Yukon River (Canada/USA) is due to the increase of groundwater contribution. Indeed, the permafrost thawing leads to an increase of 0.7–0.9% of the water contribution to streamflow due to more groundwater flow (infiltration and discharge) in the re-heated terrains. McClelland et al. (2004) suggest that the permafrost thawing is a possible driver for the increasing discharge from Eurasian rivers to the Arctic Ocean.
2. *Glacier tongues flowing into the sea*. Jaquet and Siegel (2003) studied the impact of the thawing of local glacier tongues in a marine intrusion setting in the Scandinavian shield. As for the above continental-scale studies, Jaquet and Siegel (2003) hypothesized the presence of eskers, sufficient hydraulic conductivity and permafrost with limited extension. In this case, infiltration rates were as high as 50 mm/year.
3. *Cirque and valley glaciers*. Most of the glaciers in the northwest Alps are cirque glaciers and valley glaciers. In former permafrost zones or in zones where the thick basal till (essentially clays) has disappeared, present-day (or interglacial) infiltration rates are generally between 200 and 800 mm/year (Maréchal 1998; Gallino 2007; Thiébaud 2008). As the widely accepted glacial-period infiltration rates noted above are so much lower than the infiltration rates measured during interglacial periods, glacial-period infiltration values can be considered negligible.

The objective of the present study was to determine the effect of paleoclimatic events, in particular the Quaternary glacial cycle and the resulting advance and retreat of valley glaciers, on the presence of thermal outlets and on the temperature of the waters at these outlets. The thermal outlets of Aix-les-Bains were selected for this hydrodynamic–thermal modeling for two main reasons:

1. The geometry of the reservoir is well known from deep geophysical data.
2. Monitoring of the physical parameters (flow rate, temperature, electrical conductivity) of springs and wells has provided detailed knowledge of the hydrodynamic behavior of the aquifer.

Geographical setting

Aix-les-Bains is a spa town on the eastern shore of Lake Bourget in the Savoie region of France (Fig. 1a). The town lies at an altitude of 230 m above sea level (asl; Fig. 1b). Sulfurous and HCO_3 SO_4-calcareous waters emerge from two natural sources: the Alun and Soufre springs (Fig. 1c). Discharge temperatures for the two springs are approximately 40°C and their flow rates are 20 and 17 L/s, respectively. At present, two deep boreholes supply the thermal baths with water. The Reine Hortense borehole draws its water at a depth of 1,100 m and a temperature of 37°C and the Chevalley borehole draws its water at a depth of 2,200 m and a temperature of 75°C.

Geological setting and flow pattern

The study area lies between the most southerly point of the Jura Range and the sub-alpine Bauges Mountains, at the southwest end of the molassic basin that extends from Chambery (France) to Linz (Austria) (Fig. 2a). The Aix-les-Bains geological series consists mainly of limestones with some marl intercalations (Carfantan 1992), which act as regional aquicludes. The limestones are generally karstified and form aquifers. Some large east-dipping thrust faults mean that the units to the east overlap the units to the west (Butler 1992). These thrust zones, which include evaporitic rocks, act as both hydrodynamic drains and mineralizers.

The study area consists of a succession of faults that have thrust anticlines (Montagne de la Charvaz, Mont du Corsuet) over synclines (Lake Bourget syncline) (Fig. 1b and 2b). The infiltration zone is in the Upper Tithonian to Valanginian limestones of the Montagne de la Charvaz, on the west side of Lake Bourget. This is the only catchment area in the study area to show a water deficit. Perennial water levels along this infiltration zone are known (e.g. Le Golet de la Loubatière). These water levels indicate the maximum head available for the thermal aquifer. Due to the overlying Hauterivian marls and the synclinal structure of Lake Bourget, the infiltration waters percolate down to

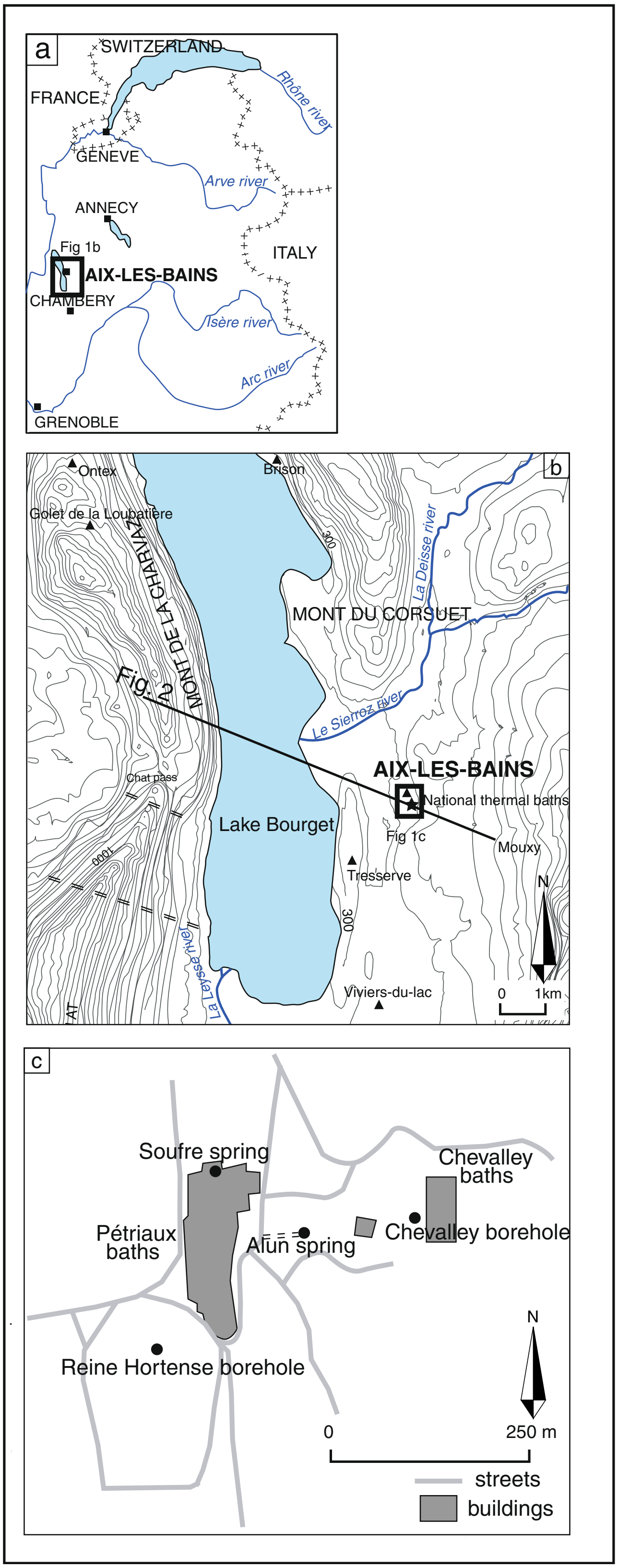

Fig. 1 Location of the study area. **a** Regional map; **b** local map; **c** location of the thermal outlets. Elevation contours are at 50-m intervals, in meters above sea level

a depth of 2,200 m. They then follow the fault plane along which the Aix-les-Bains anticlinal dome has been thrust over the Lake Bourget syncline, becoming mineralized with Cl, SO_4, Na and K ions. Below Aix-les-Bains, the mineralized waters enter a series of vertical fractures that crosscut all the beds of the Aix-les-Bains dome (from Upper Tithonian to Barremian). The waters rise through these fractures too fast for them to achieve thermal equilibrium with the surrounding rock; however, the dissolved sulfates in the waters are reduced to sulfides by bacterial action (Gallino et al. 2008). As they approach the surface, the thermal waters flow through the Barremian karst that marks the most recent layer of the Aix-les-Bains anticlinal dome. The karst network disperses the flow of the thermal waters, causing them to mix with surface karst waters.

Hydrodynamic–thermal modeling

Calculations were performed using the FEFLOW groundwater finite-element simulator (Diersch 1996). First, a hydrodynamic calibration was carried out in order to define the hydrodynamic parameters (hydraulic conductivity, storage coefficient). This then enabled thermal calibration to be carried out.

Governing equations

The groundwater flow and associated transfers (mass and/or temperature) are governed by the conservation equations. The general equation expresses the relationship between the storage capacity M (kg/m^3), the flow gradient F (kg/m^2/s) and the source S (kg/m^3/s; Wang and Anderson 1982; Domenico and Schwartz 1997; Kovarik 2000):

$$\frac{\partial M}{\partial t} = -\nabla.F + S \qquad (1)$$

The mass conservation equation for the variable density fluid phase incorporates the fluid density ρ (kg/m^3), medium porosity φ (-), Darcy velocity q (m/s), fluid expansion coefficient β (1/K), temperature T (K) and the source term i:

$$\frac{\partial(\rho\varphi)}{\partial t} = -\nabla.(\rho q) + \left(\varphi\beta\frac{\partial T}{\partial t} + q\frac{\partial T}{\partial x}\right) \pm i \qquad (2)$$

Note that q equals:

$$q = -K_0\frac{\mu_0}{\mu}\left(\nabla h + \frac{\rho - \rho_0}{\rho_0}\nabla z\right) \qquad (3)$$

where K_0 = the hydraulic conductivity tensor (m/s), μ_0 = reference viscosity, μ = effective viscosity, h = head (m), ρ_0 = reference fluid density, ρ = effective fluid density (kg/m^3) and ∇z = gravitational unit vector (m).

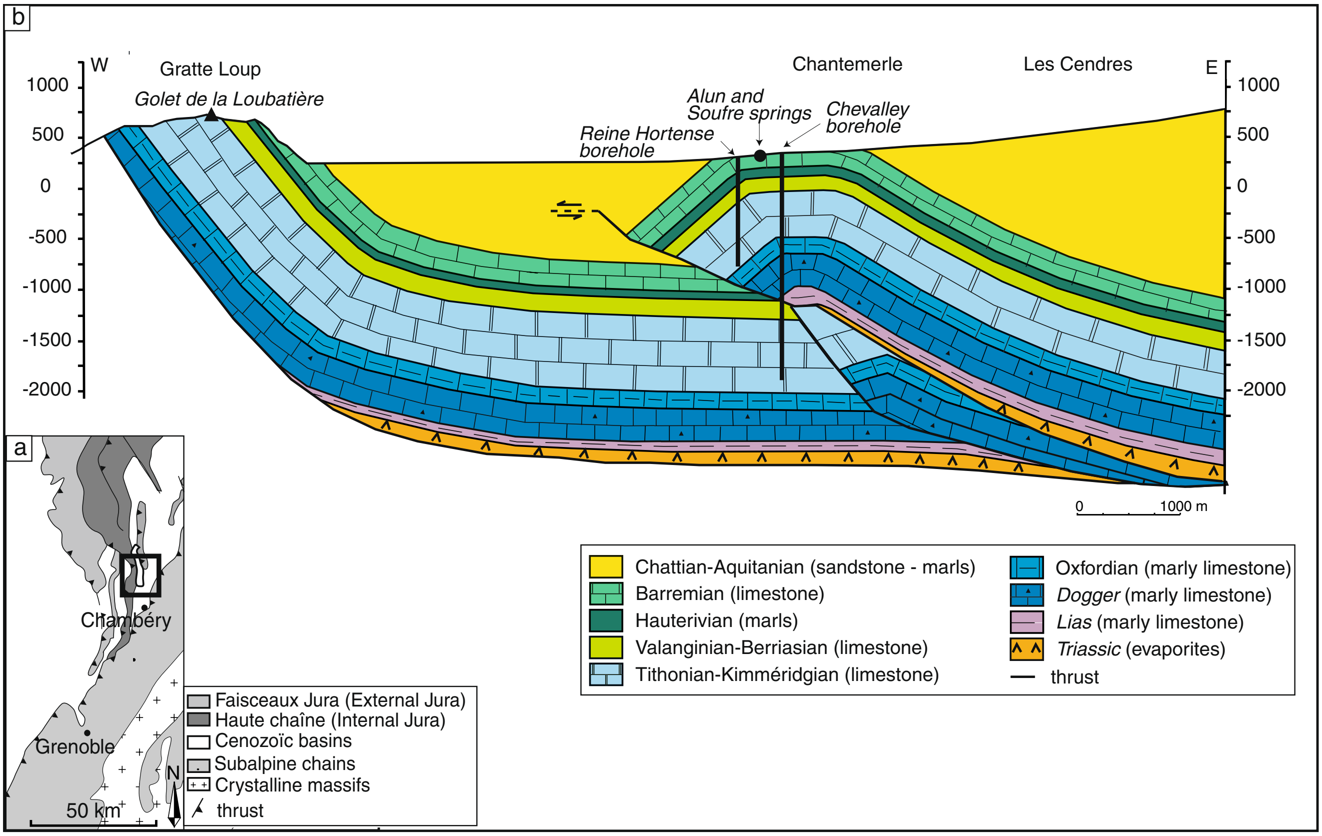

Fig. 2 Geological setting of the study area. **a** Regional structural diagram; **b** circulation diagram for Aix-les-Bains' thermal waters

The conservation equation, Eq. (1), for advective-dispersive-diffusive transport of thermal energy is:

$$\frac{\partial\left[(\varphi\rho_C)_L + (1-\varphi)(\rho_C)_S\right]T}{\partial t} = -\nabla\left[(\rho_C)_L qT - \Lambda\nabla T\right] \quad (4)$$

where ρ_{CL} and ρ_{CS} are the volumetric heat capacities (J/m^3/K) of the liquid and solid phases respectively, Λ is the hydrodynamic thermal dispersion tensor of the fluid (J/m/s/K), T is the temperature (K) and q is the parameter defined in Eq. (3).

Geometry and meshing

A vertical flow model was constructed for a 9-km cross section from the Montagne de la Charvaz to Mouxy via Les Thermes Nationaux (Fig. 1b). The geometry of the geological structures was assumed to remain unchanged from north to south (i.e. geological structures present in the west–east cross sections remain homogeneous from north to south).

A mesh with triangular elements was generated using the "T-mesh" generator developed by Ferrer (2001) at EPF Lausanne. For the present study, the mesh was refined along the thrust between the Aix-les-Bains anticline and the Lake Bourget syncline so that the strong hydraulic gradients in this sector did not generate calculation errors (Fig. 3).

The final model had 46,167 elements for a 9-km long and 5,300-m high superelement. The polygons representing the aquifer had mean surface areas of about 1,000 m^2. The quality of the mesh was estimated by calculating the percentage of triangles with obtuse angles and the percentage of triangles that did not comply with the Delaunay criterion (i.e. the circumcircle of a triangle must not contain the apex of another triangle). In the case of the Aix-les-Bains model, these triangles accounted for only 7.5 and 4.2% of all triangles, respectively, which is acceptable.

Boundary conditions of the hydrodynamic model

The boundary conditions are the inflow fluxes and the constrained heads at the springs (Fig. 3). In the case of deepwater aquifers in regions with high relief, Sanford (2002) advises representing the infiltration flow by a flux boundary condition. The inflow due to effective rainfall (i.e. total rainfall minus evapotranspiration) was assigned a value of 1.8 mm/d (average of recordings made as part of this study between June 2006 and June 2007). The infiltration area does not show any evidence of surface runoff or gullies; hence, it was assumed that the infiltration rate was equal to the effective rainfall. The 2D model represents a 1-m wide slice through the aquifer, which led

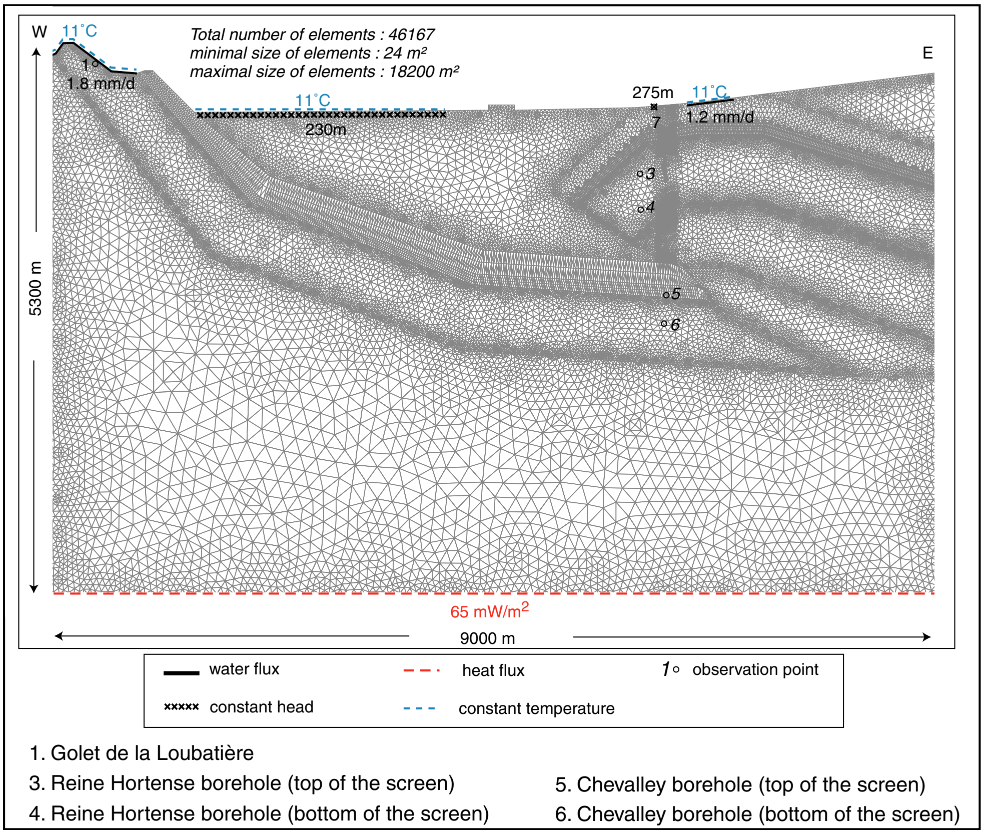

Fig. 3 Meshing and boundary conditions for the 2D model. Observation points Nos. *3*, *4*, *5* and *6* are used for comparison with present-day heads and temperature values, obtained from measures performed between drilling and groundwater production

to division of the flows by the width of the aquifer (4,500 m in the case of Aix-les-Bains).

Calibration of the hydrodynamic model

The hydrodynamic calibration, made by trial and error, was considered satisfactory when the heads at the observation points closely matched the flow and head data, especially for observation point number 1 (Table 1), when the flow rates at the springs were similar to the observed flow rates, when the residence time was millennial, and when the hydraulic conductivities of the different geological units corresponded to known magnitudes, especially for the impermeable formations.

The robustness of the model was also tested by increasing the number of elements in order to ensure that charges were not simulated using erroneous calculations resulting from insufficiently fine meshing. The calibration (Table 1) produced a field of anisotropic hydraulic conductivities. These conductivities were stronger parallel to the layers than perpendicular to them. The result was a field of hydraulic conductivities Kmax (m/s) along stratigraphic joints, with anisotropy between Kmax and Kmin and with an angle between the x-axis and Kmax (Fig. 4).

The average transfer velocity for the whole aquifer (Tithonian to Valanginian series) was $1.2{\cdot}10^{-3}$ m/d. Assuming a porosity of 0.06, this indicates a true velocity of 0.02 m/d. As the distance between the infiltration area and the deep borehole is approximately 7,200 m, the

Table 1 Summary of observed and simulated heads and/or flow rates

Site	Observation point	Observed head/flow rates	Simulated head/flow rates
Reine Hortense (top screen)	3	275 m (artesian head)	283 m (artesian head)
Reine Hortense (bottom screen)	4		
Chevalley (top screen)	5	314 m (artesian head)	317 m (artesian head)
Chevalley (bottom screen)	6		
Alun and Soufre springs	7	275 m[a]/45 L/s	275 m[a]/46 L/s
Golet de la Loubatière	1	715 m	735 m

[a] Refers to the values imposed on the model

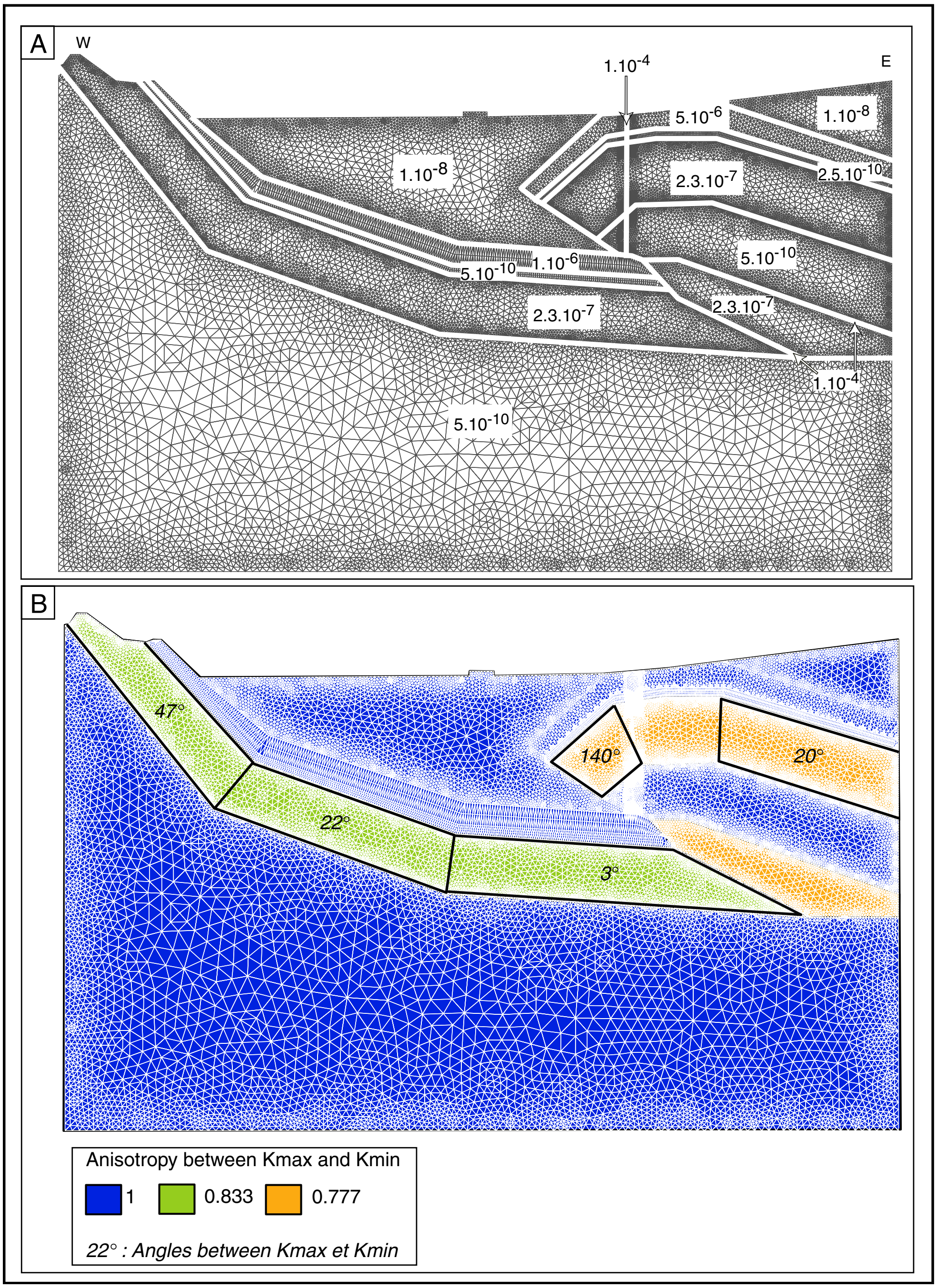

Fig. 4 Hydrodynamic calibration of the model: **a** hydraulic conductivity (Kmax) field. **b** Anisotropy factor between Kmax and Kmin and angles between x-axis and Kmax (counterclockwise direction). If values are not precise, angles between Kmax and Kmin are taken to be equal to zero

transfer time between the infiltration area and the Chevalley borehole is about 1,000 years. Such a transfer time is in agreement with transfer times calculated using geochemical data.

Parameters of the thermal model

A geothermal flux of 65 mW/m^2 was specified at the bottom of the model (Lucazeau and Vasseur 1988). This value is the mean of the flows measured in two oil exploration boreholes drilled by Esso Rep (1976) north of Aix-les-Bains (Fig. 3). A temperature of 11°C was assumed for the infiltration zone and for the lake surface. This temperature, the mean annual temperature of the study area, was associated with the infiltration flow of the model.

The heat capacity and thermal conductivity of the rocks and the water were uniform throughout the mesh. The FEFLOW default heat capacity value ($2.52{\cdot}10^6$ J/m^3/K) was used for the solid phase, as the literature indicates values of around $2.43 \cdot 10^6$ J/m^3/K for limestones and $2.52 \cdot 10^6$ J/m^3/K for dolomites (Waples and Waples 2004). As several authors (Özkahraman et al. 2004; Pfingsten et al. 2001) have reported mean solid thermal conductivity values of 2 W/m/K for limestones, this value was used in the present study. FEFLOW default values were used for the thermal conductivity (0.65 W/m/K) and heat capacity ($4.2 \cdot 10^6$ J/m^3/K) of water.

Summary of the functioning hypothesis

The first simulation was carried out with the boundary conditions shown in Table 2.

Results and discussion

Calibration with the current functioning hypothesis

The temperature distribution at the beginning of the simulation (using current thermal limit conditions) was obtained by applying a geothermal flux of 65 mW/m^2 to the base of the model and assuming no water circulation. A geothermal flux of 65 mW/m^2 and no water circulation produces a thermal steady state that results in a geothermal gradient of 1°C/23 m.

With this initial state, if the aquifer functions with the current hydrodynamic and thermal limit conditions (see Table 2), the rock mass would cool and the geothermal flux would not be high enough to heat the waters (Fig. 5). Maintaining these conditions would result in a new thermal equilibrium being reached after a period of 600,000 years.

The hydrodynamic functioning of the system would generate a large thermal imbalance that cannot be compensated for by modifying the thermal parameters of the model (heat capacity, thermal conductivity) without moving a long way from the values generally accepted in the literature (see the preceding section Parameters of the thermal model). This thermal imbalance can only be reduced by reducing the input of water; that is to say, for the geothermal flux to heat the water, the infiltration rate must be ten times lower than the present-day infiltration rate. The outlet flow rates at Aix-les-Bains would have to be no higher than 4 to 5 L/s, thereby suggesting that the previously accepted assumption that the waters are warmed as they percolate to depth (Moret 1946; Curt and Lamotte (2004); Vigouroux 2005) is only true for very low flows. The current cooling of the rock mass and the need to reduce infiltration rates by 90% to conserve the thermal balance led to the following hypothesis:

– Current infiltration rates and geothermal flux values are not representative of the entire functioning time of the aquifer.

The following scenarios can therefore be envisaged:

1. The system is younger than first thought. Steady-state functioning of the aquifer with present-day flow rates is only compatible with current water outlet temperatures if the aquifer has only functioned for approximately 10,000 years. As the porous part of the aquifer outcrops, it must necessarily have acted as an infiltration zone. Therefore, the aquifer could only have been prevented from functioning by an impermeable feature in the fractured part of the aquifer. For the aquifer to have begun functioning 10,000 years ago, the impermeable layer would have to have been opened at this time by the effects of a neotectonic event. Such events have occurred, as is shown by evidence of earthquake activity recorded in Lake Bourget sediments, but only at much older or much younger dates than 10,000 years BP (Chapron et al. 1996). Consequently, the tectonic explanation for aquifer functioning was rejected.
2. The system has functioned continuously but inflows have varied over time. In this scenario, it is necessary to invoke variable inflows as the present-day inflow would lead to excessive cooling of the entire rock mass.
3. The system has functioned intermittently. Aquifer functioning may have been blocked during the last glacial maximum by permafrost and subglacial tills. Reduced inflows and/or the inability of flows to reach outlets would block the hydrodynamic system, allowing the geothermal flux to reheat the almost stationary waters and the surrounding rocks. During interglacial periods, when the permafrost melts and the glacial tills are leached, cold water can once again seep into the aquifer and springs can reactivate. The new inflow of cold water would lead to an increase in pressure that would flush out the warmed waters. This would allow water to percolate through the aquifer and gradually cool the rock mass until a new blocked phase occurs.

Two series of simulations were performed, one to test the effect of changes in inflow rate on outlet temperatures and the second to test the thermal consequences of a hydrodynamic blocked phase.

Influence of inflow on the final thermal state

Hypothesis

As for the simulations described in the preceding paragraphs, the tests examining the influence of variations in

Table 2 Imposed parameters and observed values for the first simulation

Imposed values	Hydrodynamic parameters	Inflow: 1.8 mm/d (Tithonian-Valanginian limestone) and 1.2 mm/d (Barremian limestone) Outflow: constant head (275 m asl)
	Thermal parameters	Inflow: 11°C Geothermal flux: 65 mW/m^2
Observed values	Hydrodynamic parameters	Flow rates at the springs and artesian heads at wells
	Thermal parameters	Temperatures at the springs and at the wells

Fig. 5 Thermal evolution (contours in 10° intervals) of the model at different stages of aquifer functioning for an inflow of 1.8 mm/d

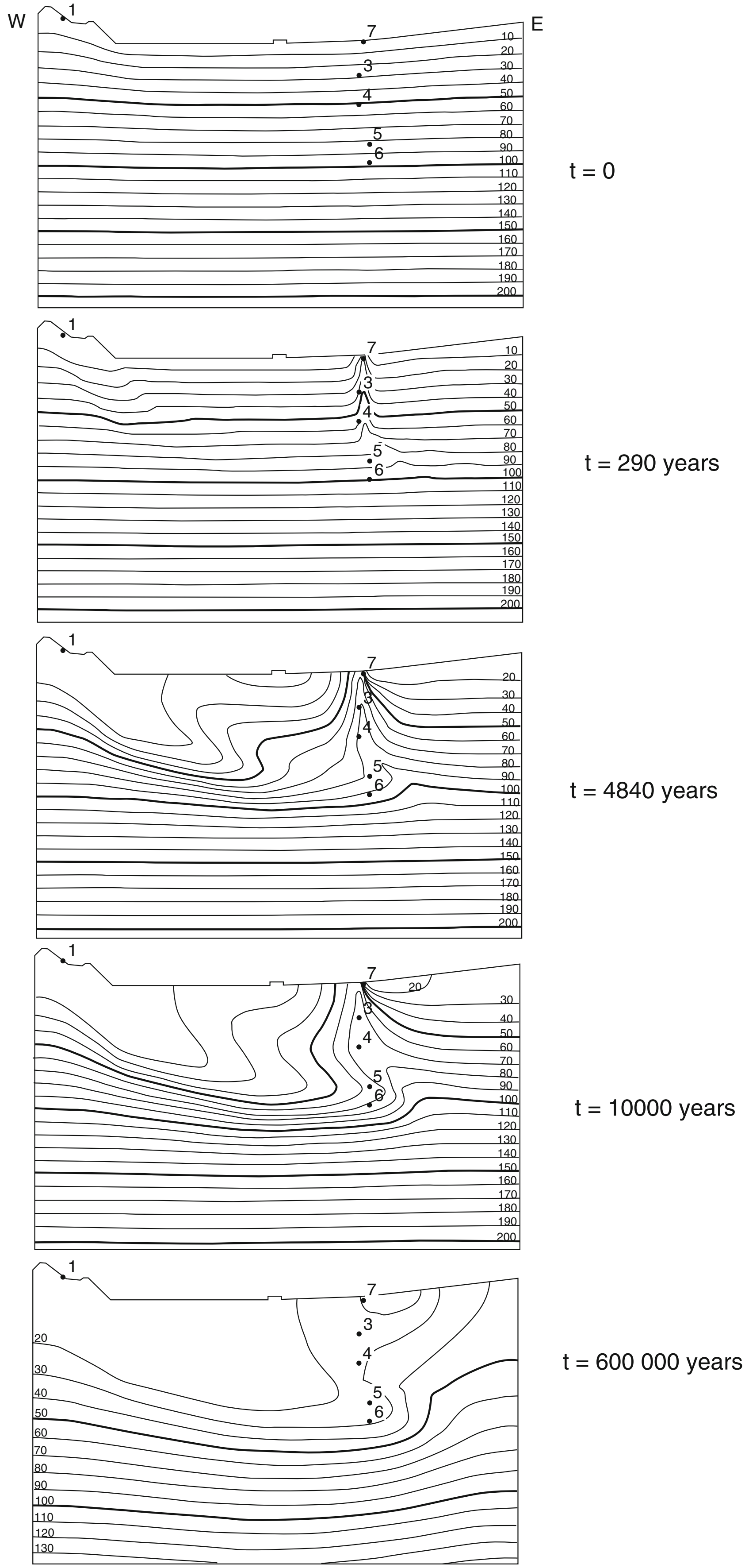

inflow were carried out assuming that the aquifer started functioning after the last glaciations and that the initial thermal conditions were obtained during a long period without flow. The dating of the glaciation and deglaciation phases is still the subject of debate. Some authors believe that glacier retreat following the Würmian glaciation in the western part of the Northern Alps started 10,000 years ago (e.g. Preusser et al. 2003). Others (e.g. Guiter et al. 2005) maintain that glacier retreat began 20,000 years ago. Due to Aix-les-Bains' location on the margin of the glaciated area, this study assumes that glacier retreat began 20,000 years ago.

One possible explanation for the inconsistency between present-day temperatures and aquifer cooling is variations in aquifer inflow leading to changes in the intensity of flushing. Simulations were conducted to determine how changes in inflow rate impact outlet temperatures.

Tests

For the first simulation an input to the infiltration area of 1.8 mm/d was assumed for a period of 20,000 years (as for the Aix-les-Bains model in the preceding section Calibration with the current functioning hypothesis). This gives a total infiltration volume of 13,140 m^3/m^2 of aquifer. The resulting temperatures served as a reference for the subsequent simulations. Maintaining a functioning period of 20,000 years, the effects of higher and lower infiltration volumes were simulated next (Table 3).

Changes in infiltration volume lead to changes in outlet temperature, with temperatures first reaching a maximum and then decreasing according to a power law (Fig. 6). Once the maximum temperature has been reached, the higher the cold inflow, the greater the effect of flushing towards the outlets. The lowest temperatures are observed before the maximum temperature peak because the inflow at this juncture is too low to have flushed through the deeper and warmer waters. The absolute value of the maximum temperature at the outlet and the volume required to reach this maximum temperature depend on the geometry of the aquifer. The temperatures currently observed at the Aix-les-Bains outlets are compatible with

Table 3 Outlet temperatures with different infiltrated volumes and flow rates

Flow rate (mm/d^1)	Infiltrated volume (m^3/m^2 of aquifer)	Temperature at the outlet (°C)
0.5	3,650	40
1.0	7,300	48.8
1.2	8,760	46.3
1.4	10,220	42.3
1.6	11,680	38.2
1.8[a]	13,140[a]	34.5[a]
2.0	14,600	31.4
2.2	16,060	28.9
2.4	17,520	26.7
3.5	25,550	19.6
4.0	29,200	17.9

[a] Represents both the flow rate measured on the field and the flow rate used in the first simulation

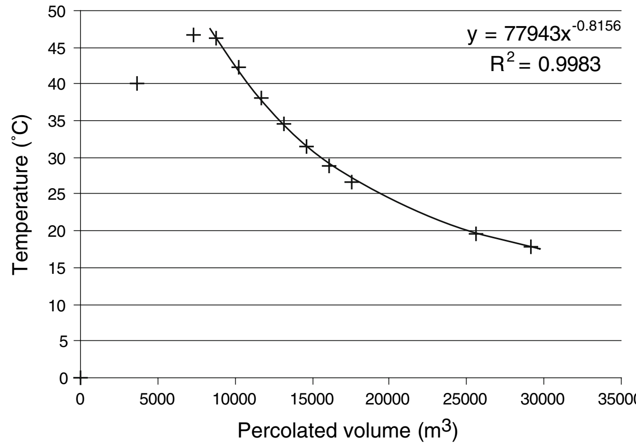

Fig. 6 Temperature evolution at the outlet in terms of total infiltrated volumes

a mean inflow of between 1.2 and 1.6 mm/d over a period of 20,000 years, a value that is much lower than the 1.8 mm/d currently measured.

After testing the effect of variations in flow intensity, the influence of a succession of inflows was tested for a constant total infiltration volume (Table 4). As the current inflow of 1.8 mm/d is too high to explain the measured cooling, the 20,000-year period was divided into three successive inflow episodes with the following characteristics:

- An episode with an inflow of a third the current value
- An episode with an inflow of two-thirds the current value
- An episode with an inflow equal to the current value

This gave a mean inflow value of 1.2 mm/d, a value that was used as the reference value for this series of simulations.

The three cases simulated were: 1.2 mm/d for 20,000 years; successive episodes of 0.6, 1.2 and 1.8 mm/d, each lasting 6,666 years; and successive episodes of 1.2, 0.6 and 1.8 mm/d, each lasting 6,666 years. The resulting outlet temperatures were similar in each case. As the total infiltrated volumes were identical, the flushing effect was the same in all three cases, leading to the same thermal evolution of the aquifer. Variations in inflow rate do not influence final outlet temperatures, if the total infiltrated volume is constant.

Influence of a blocked hydrodynamic phase on the thermal state of the aquifer

The second hypothesis for explaining the outlet temperatures of Aix-les-Bains' thermal springs is that the system has only functioned intermittently. Given a fixed functioning period, several simulations were carried out to determine how long the blocked period (no inflow or outflow) would have to be for the aquifer to return to its initial thermal state (similar to t=0 in Fig. 5). Functioning times of between 5,000 and 30,000 years were tested, with an inflow of 1.8 mm/d (the present-day inflow). The time needed for a hydrodynamically blocked system to return

Table 4 Outlet temperatures with variable inflow rates but a constant total infiltration volume

Flow rate (mm/d)	Length (years)	Percolated volume (m^{3}/m^{2} of aquifer)	Temperature at the outlet (°C)
1.2	20,000	8,760	46.3
0.6	6,666	8,760	47.2
1.2	6,666		
1.8	6,666		
1.2	6,666	8,760	48.6
0.6	6,666		
1.8	6,666		

to an undisturbed gradient increases as the length of the functioning period increases (Table 5).

Similarity between the rhythms of the blocked/functioning phases and of the Quaternary glaciations/deglaciations

The correspondence between the rhythms of the blocked/functioning phases and of the Quaternary glaciations/deglaciations is based on two observations.

1. A hydrodynamic regime consisting of alternating blocked periods and functioning periods is compatible with the features of the Quaternary glaciation. Glaciation results in the deposition of compacted and impermeable subglacial tills (mostly clay) in valley bottoms, and to the formation of permafrost on the upper flanks of valleys and on ridgelines (Chapron 1999). These two phenomena significantly reduce or completely block aquifer inflows and/or outlets. The flushing effect described in the preceding section Calibration with the current functioning hypothesis is substantially reduced, thus modifying the hydrodynamic state of the aquifer. However, as glaciation does not change geothermal fluxes, the thermal state of the aquifer is also modified. In contrast, deglaciation will once again allow the aquifer to be infiltrated by inflows (erosion of the impermeable subglacial till), which then generate the flushing effect described above.
2. The lengths of the blocked and functioning periods indicated by the simulations described in the preceding section Influence of a blocked hydrodynamic phase on the thermal state of the aquifer are similar to the lengths of the Quaternary glaciations and deglaciations (Table 6).

Table 5 Blocked periods required following different functioning periods

Operating time period (years)	Required blocked period (years)
5,000	5,000–10,000
10,000	20,000–30,000
15,000	30,000–50,000
20,000	70,000–80,000
30,000	180,000–200,000

The simulation of how the Aix-les-Bains thermal system would have been affected by a succession of blocked and functioning phases of similar lengths to the Quaternary glacial and interglacial periods required one to make a number of approximations:

– Although pollen analyses have indicated variations in temperature and rainfall for the different glacial and interglacial periods (Drescher-Schneider 2000; Peyron et al. 1998), inflows were assumed to be similar to present-day flow rates (1.8 mm/d).

Table 6 Dating and duration of Quaternary glacial and interglacial periods

Glaciation period (G)/ interglacial period (IG)	Absolute dating (Ma ago)	Length (Ma)
(IG) Donau-Günz	−1,800,000/−1,200,000	600,000
(G) Günz	−1,200,000/−700,000	500,000
(IG) Günz-Mindel	−700,000/−650,000	50,000
(G) Mindel	−650,000/−350,000	300,000
(IG) Mindel-Riss	−350,000/−300,000	50,000
(G) Riss	−300,000/−120,000	180,000
(IG) Riss-Würm	−120,000/−80,000	40,000
(G) Würm	−80,000/−10,300	69,700
(IG) post Würm	−10,300/0	10,000–20,000

Ma million years

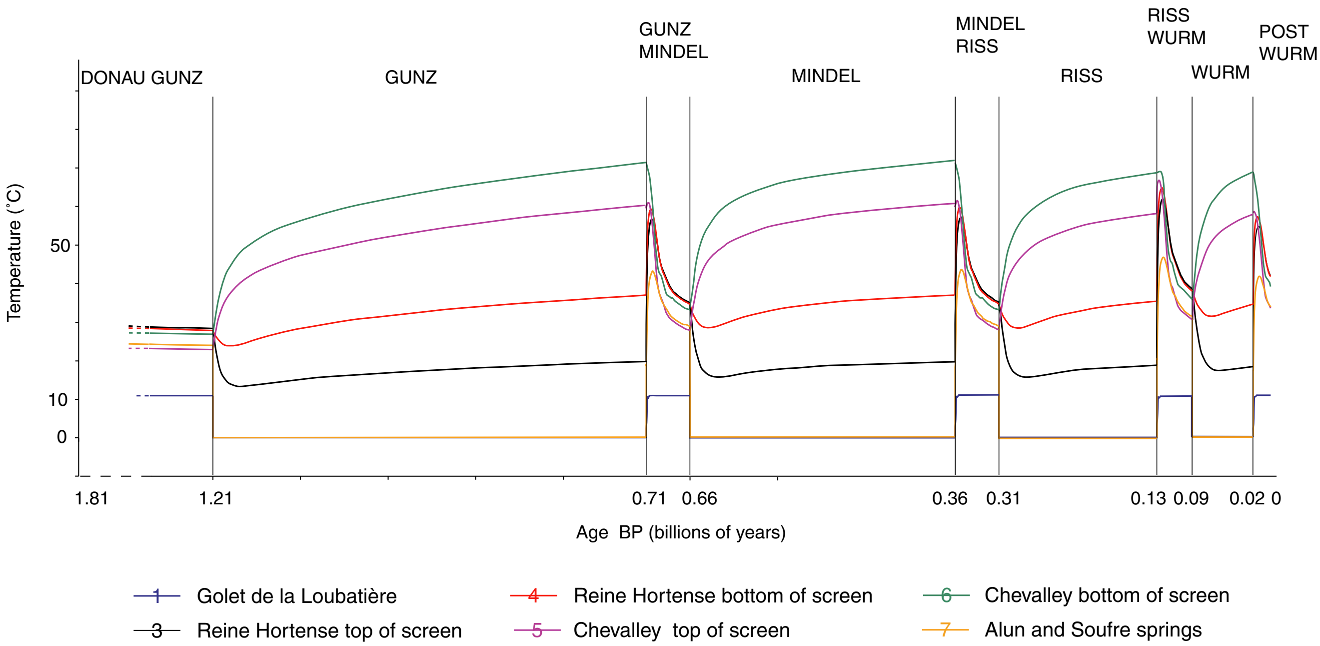

Fig. 7 Temperature evolution at different observation points during the Quaternary glaciations and deglaciations

– The lengths of the glacial and interglacial periods were calculated from ^{18}O values for icecaps at the poles. However, these data may not accurately reflect the situation in the Alps, especially in marginal locations such as Aix-les-Bains. In addition, the time needed to erode the subglacial till deposited during a glacial period may increase the length of the blocked phase.
– Although successive glaciations lead to deepening of the hydrodynamic base level, the hydrodynamic base level was assumed to be the same as the present base level.

The initial temperature field was assumed to be equal to the stabilized thermal conditions obtained after a long period of functioning (Fig. 5, t=600,000 years). In fact, the Donau-Günz interglacial period was long enough (600,000 years) for the system to cool completely. Current temperature (11°C) and flow (1.8 mm/d) conditions were applied during the interglacial phases. Inflow during the glacial phases was assumed to be zero, the surface temperature was assumed to be 0°C and the geothermal flux remained unchanged (Fig. 7).

During the first functioning period, which corresponds to the Donau-Günz interglacial period, the aquifer would have cooled completely. During glaciations, that is to say when the aquifer was blocked, the cooled water would have reheated, even if the geothermal gradient was lower than the gradient reached after a long period without flow (Fig. 8). In fact, the simulations show that geothermal gradients gradually decrease with successive glaciations. For example, after a long period without water flow, the geothermal gradient would be expected to be 1°C/23 m. During the Günz and Mindel glaciations the thermal gradient reheating the water was 1°C/30 m, a value that fell to 1°C/33 m at the end of the Riss and Würm glaciations. During functioning phases, the flow of water disrupted the geothermal gradient in the Tithonian-Valanginian layers. Geothermal gradients were also disrupted, to varying degrees, in the sections above (gradient near zero or even reversed in some cases) and below (between 2,200 and 3,800 m deep) these Tithonian-Valanginian layers (Fig. 8). The depth of disturbance is consistent with that obtained in a single functioning phase.

Conclusions

Present-day outlet temperatures for the Aix-les-Bains aquifer are incompatible with current functioning conditions (an inflow temperature of 11°C at the infiltration area and a geothermal flux of 65 mW/m^2), as the current inflow rate of 1.8 mm/d would lead to excessive cooling of the entire aquifer. Outlet temperatures indicate an average inflow rate ten times lower than the measured rate.

Thus, the current temperature field suggests that either the aquifer only started functioning relatively recently or that current conditions are not representative of the entire history of the aquifer. As there is no evidence of a major event (neotectonics during the relevant period) that could have triggered aquifer functioning, one is left to conclude that the system has functioned for a long period of time with boundary conditions that were different from current conditions, or that the system has alternated between functioning and blocked phases. Similar conclusions about the unrepresentative nature of present-day boundary conditions and the necessity to take into account the long equilibration time have been found for the Canadian Shield (Lemieux et al. 2008b).

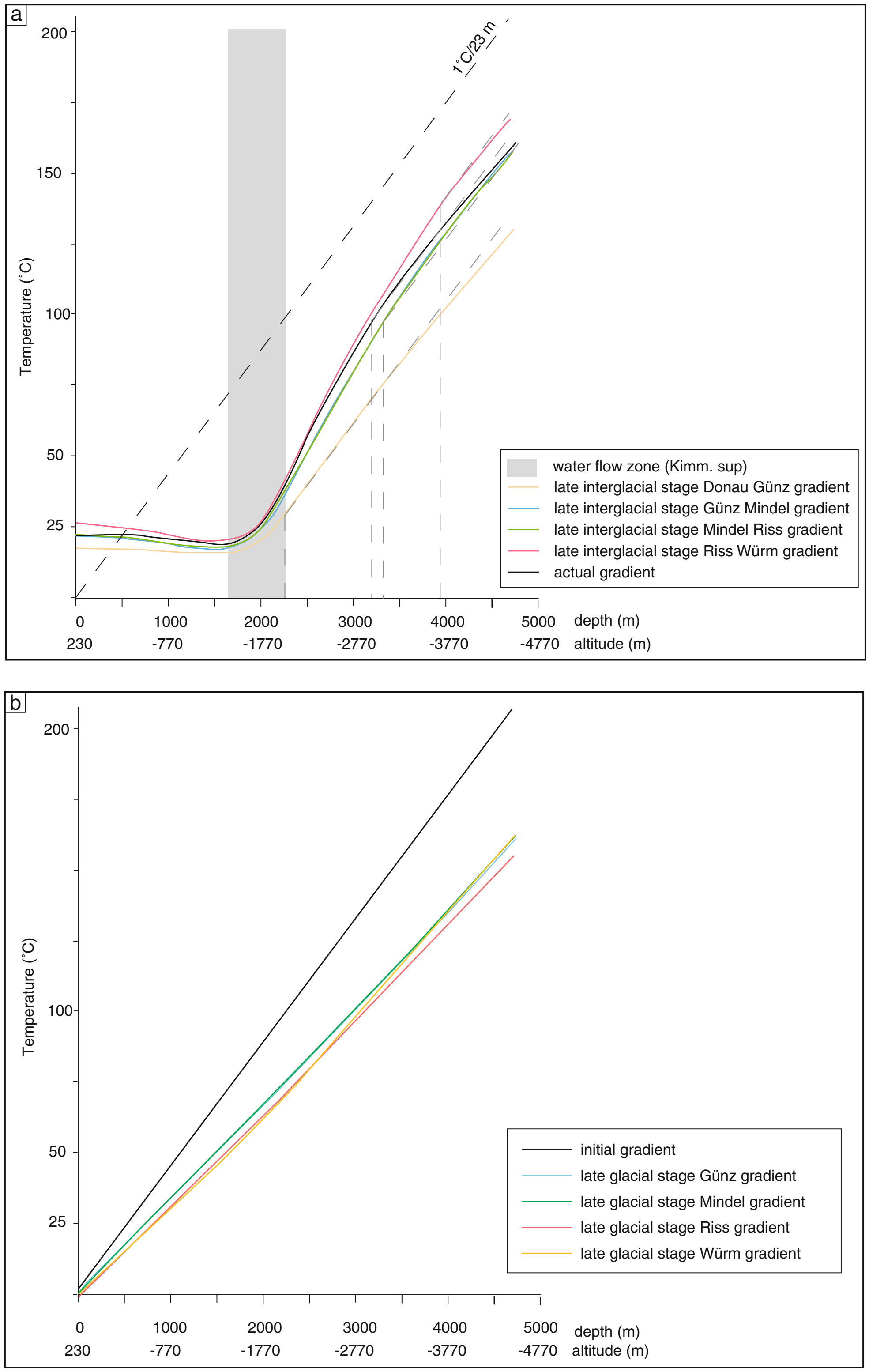

Fig. 8 Geothermal gradient evolution: **a** at the end of deglaciation periods, **b** at the end of glaciation periods

The simulations showed that:

– The current temperature field can be explained by variations in infiltration rates. These variations are compatible with the rhythm of Quaternary glaciations and deglaciations if it is assumed that there was no flow through the aquifer during glacial periods and that flow occurred during interglacial periods.
– Outlet temperatures depend on the degree of aquifer flushing induced by inflows. In this respect, the total

infiltration volume over a given period is more important than individual inflow rates.

The occurrence of blocked periods and functioning periods related to glaciations and deglaciations is a possible explanation for the temperature of the thermal springs at Aix-les-Bains. The intensity of inflows has an impact on the temperature of the outlets, and this intensity is linked to the volume of water that infiltrates the aquifer during each functioning phase.

Nevertheless, these simulations remain a first approach to the phenomenon and more information is needed about a number of parameters. For example, approximate values are available for the boundary conditions (temperature and inflow rate) at the end of the last interglacial period, but these parameters are less well known for interglacial periods prior to the Würmian glaciation. Similarly, the durations of the blocked and functioning phases have been calculated for the entire Alpine massif, but there is less information for the area investigated by the present study. Furthermore, the hydraulic conductivity of carbonate aquifers such as the Aix-les-Bains aquifer is likely to be affected by karst network development, which depends on paleoclimatic conditions.

The accuracy of the approximations made for the boundary conditions, for the timing of the blocked and functioning phases and for the hydraulic conductivities could be increased using the following tools:

- Local speleothems or lake sediment archives could be used to determine past climatic conditions
- Mapping and dating of tills in the study area would provide information on the system's blocked and functioning periods
- A karst network development model for the Tithonian-Valanginian limestone strata in the study area could be used to simulate the evolution of the aquifer's hydraulic conductivity

Acknowledgements we are grateful to J. Fairley and M. Person for the constructive review, which helped to improve the quality of the manuscript. This research has been financially supported by three companies of Aix-les-Bains (Thermes Nationaux, Thermes de Marlioz, Société des Eaux d'Aix-les-Bains).

References

Bense VF, Person MA (2008) Transient hydrodynamics within intercratonic sedimentary basins during glacial cycles. J Geophys Res 113, F04005. doi:10.1029/2007JF000969

Boulton GS, Caban PE, Van Gijssel K, Leijnse A, Punkari M, Van Weert FHA (1996) The impact of glaciation of the groundwater regime of Northwest Europe. Glob Planet Change 12(1–4):397–413

Bredehoeft JD, Papadopulos IS (1965) Rates of vertical groundwater movement estimated from the Earth's thermal profile. Water Resour Res 1(2):325–328

Butler RWF (1992) Structural evolution of the western Chartreuse fold-and-thrust system, NW French Subalpine chains. In: Mc Clay KR (ed) Thrust tectonics. Chapman and Hall, London, pp 287–298

Carfantan J-C (1992) Petit guide de la géologie régionale [Guide of the regional geology]. Internal report, LGHAM, Université de Savoie, Chambery, France

Chapron E (1999) Contrôles climatiques et sismo-tectonique de la sédimentation lacustre dans l'avant pays alpin (Lac du Bourget) durant le Quaternaire récent [Climatic and seismo-tectonic control on late Quaternary lacustrine sedimentation in the alpine foreland (Le Bourget and Geneva lakes)]. PhD Thesis, Université de Grenoble, France, Mémoire de Géologie Alpine H.S. No. 30, 261 pp

Chapron E, Vanrensbergen P, Beck C, De Batist M, Paillet A (1996) Lacustrine sedimentary records of brutal events in Lake Le Bourget (Northwestern Alps-Southern Jura). Quaternaire 7(2–3): 155–168

Curt AL, Lamotte C (2004) Ressource en eau thermale de la station d'Aix-les-Bains. [Thermal water resources of Aix-les-Bains thermal spa]. Final report, BRGM RP-52859-FR, BRGM, Orleans, France, 119 pp

Diersch HJ (1996) Interactive, graphic-based finite element simulation system FEFLOW for modeling groundwater flow, contaminant mass and heat transport processes. Wasy, Berlin

Domenico PA, Schwartz FW (1997) Physical and chemical hydrogeology, 2nd edn. Wiley, New York, 506 pp

Drescher-Schneider R (2000) The Riss-Würm interglacial from West to East in the Alps: an overview of the vegetational succession and climatic development. Geol Mijnbouw 79(2–3): 233–239

Durand V (2005) Recherche multidisciplinaire pour caractériser deux aquifères fracturés: les eaux minérales de Plancoët en contexte métamorphique, et de Quézac en milieu carbonaté [Multidisciplinary research to characterize two fractured aquifers: mineral waters of Plancoët in metamorphic context, and of Quézac in carbonate context]. PhD Thesis, Université Paris 6, Pierre et Marie Curie, France, 255 pp

Esso Rep (1976) Rapport de fin de sondage La Tailla 1 [Report after drilling La Tailla 1]. Esso Group , Lege Cap Ferret, France, 14 pp

Ferrer M (2001) Meshing of complex shapes in earth sciences. PhD Thesis EPFL, Switzerland, 106 pp

Gallino S (2007) Hydrogéologie, géochimie et modélisation hydrodynamique-thermique d'un système thermo-minéral associé un contact structural alpin (Aix-les-Bains - Savoie) [Hydrogeology, geochemistry and coupled hydrodynamic-thermical modeling of a thermo-mineral system associated with an alpine thrust (Aix-les-Bains, Savoie)]. PhD Thesis, Université de Savoie, France, 338 pp

Gallino S, Bulloz M, Naffrechoux E, Dzikowski M, Gasquet D (2008) The influence of extraction rate on the reduced sulphur content of Aix-les-Bains' thermal spring waters: consequences for resource-quality monitoring. Appl Geochem 23:1367–1382

Ge S, Garven G (1992) Hydromechanical modeling of tectonically driven groundwater flow with application to the Arkoma foreland basin. J Geophys Res 97:9119–9144

Guiter F, Triganon A, Andrieu-Ponela V, Ponela P, Hebrard JP, Nicoud G, De Beaulieu JL, Brewere S, Guibala F (2005) First evidence of "in situ" Eemian sediments on the high plateau of Evian (Northern Alps, France): implications for the chronology of the Last Glaciation. Quat Sci Rev 24:35–47

Jaquet O, Siegel P (2003) Groundwater flow and transport modeling during a glaciation period. SKB report R-03-04, SKB, Stockholm, 44 pp

Kovarik K (2000) Numerical models in groundwater pollution. Springer, Berlin, 221 pp

Le Fanic R (2005) Hydrogéologie d'un système thermal et modélisation couplée hydrodynamique/thermique en vue de la gestion de la ressource: application au système de Dax-Saint-Paul-lès-Dax [Heat transfer and fluid flow modeling as a management tool of thermal water ressource of the hydrothermal system of Dax, Saint-Paul-Lès-Dax (France)]. PhD Thesis, Université de Bordeaux 3, France, 285 pp

Lemieux JM, Sudicky EA, Peltier WR, Tarasov L (2008a) Dynamics of groundwater recharge and seepage over the Canadian landscape during the Wisconsinian glaciation. J Geophys Res 113, F01011. doi:10.1029/2007JF000838

Lemieux JM, Sudicky EA, Peltier WR, Tarasov L (2008b) Simulating the impact of glaciations on continental groundwater flow systems: 2. Model application to the Wisconsinian glaciation over the Canadian landscape. J Geophys Res 113, F030017. doi:10.1029/2007JF000929

Lu N, Ge S (1996) Effect of horizontal heat and fluid flow on the vertical temperature distribution in a semiconfining layer. Water Resour Res 32(5):1449–1453

Lucazeau F, Vasseur G (1988) Heat density data from France and surrounding margins. Tectonophysics 164:251–258

Mansure AJ, Relter M (1979) A vertical groundwater movement correction for heat flow. J Geophys Res 84(B7):3490–3496

Maréchal JC (1998) Les circulations d'eau dans les massifs cristallins alpins et leurs relations avec les ouvrages souterrains [Groundwater flows in the Alpine crystalline massive and their relations with underground works]. PhD Thesis, No. 1769, Ecole Polytechnique Fédéral de Lausanne, Switzerland, 296 pp

Maréchal JC, Perrochet P (1999) Long-term simulations of thermal and hydraulic characteristics in a mountain massif: the Mont-Blanc case study, French and Italian Alps. Hydrogeol J 7:341–354

Maréchal JC, Perrochet P (2001) Theoretical relation between water flow rate in a vertical fracture and rock temperature in the surrounding massif. Earth Planet Sci Lett 194(1–2):213–219

McClelland JW, Holmes RM, Peterson BJ, Stieglitz M (2004) Increasing river discharge in the Eurasian Arctic: consideration of dams, permafrost thaw, and fires as potential agents of change. J Geophys Res 109, D18102. doi:10.1029/2004JD004583

Moret L (1946) Les eaux thermominérales: hydrogéologie, géochimie, biologie [Thermomineral waters: hydrogeology, geochemistry, biology]. Masson, Paris, 146 pp

Özkahraman HT, Selver R, Işik EC (2004) Determination of the thermal conductivity rock from P-wave velocity. Int J Rock Mech Min 41(4):703–708

Person M, Toupin D, Eadington P (1995) Effects of convective heat transfer on the thermal history of sediments and petroleum generation within continental rift basins. Basin Res 7:81–96

Person M, McIntosh J, Bense V, Remenda VH (2007) Pleistocene hydrology of North America: the role of ice sheets in reorganizing groundwater flow systems. Rev Geophys 45, RG3007. doi:10.1029/2006RG000206

Peyron O, Guiot J, Cheddadi R, Tarasov P, Reille M, de Beaulieu JL, Bottema S, Andrieu V (1998) Climatic reconstruction in Europe for 18,000 YR B.P. from pollen data. Quat Res 49:183–196

Pfingsten W, Hadermann J, Perrochet P (2001) Radionucleide release and transport from nuclear underground tests performed at Mururoa and Fangataufa: predictions under uncertainity. J Contam Hydrol 47(2–4):349–363

Preusser F, Geyh MA, Schluchter C (2003) Timing of Late Pleistocene climate change in lowland Switzerland. Quat Sci Rev 22:1435–1445

Sanford W (2002) Recharge and groundwater models: an overview. Hydrogeol J 10:110–120

Thiébaud E (2008) Fonctionnement d'un système hydrothermal associé à un contact tectonique alpin (La Léchère, Savoie). Apports de l'hydrogéologie, de la géochimie et de la modélisation hydrodynamique–thermique en vue de la gestion de la ressource [Characterization of a hydrothermal system associated to an alpine tectonic contact (La Léchère, Savoie): contributions of hydrogeology, geochemistry and hydrodynamic–thermic modeling to the water resource management]. PhD Thesis, Université de Savoie, France, 330 pp

Ungerer P, Burrus J, Doligez B, Chenet PY, Bessis F (1990) Basin evaluation by integrated two-dimensional modeling of heat transfer, fluid flow, hydrocarbon generation, and migration. AAPG Bull 74(3):309–335

Vigouroux P (2005) Guide qualité pour la ressource en eau minérale et thermale [Guide for the quality of the thermal and mineral water resource]. BRGM, Orleans, 80 pp

Walvoord MA, Striegl RG (2007) Increased groundwater to stream discharge from permafrost thawing in the Yukon River basin: potential impacts on lateral export of carbon and nitrogen. Geophys Res Lett 34, L12402. doi:10.1029/2007GL030216

Wang HF, Anderson MP (1982) Introduction to groundwater modeling. Academic, San Diego, 237 pp

Wang K, Beck AE (1988) An inverse approach to heat flow study in hydrologically active areas. Geophys J Int 98(1):69–84

Waples DW, Waples JS (2004) A review and evaluation of specific heat capacities of rocks, minerales and subsurface fluids, part 1: minerals and nonporous rocks. Nat Resour Res 13(2):97–122

Woodbury AD, Smith L (1988) Simultaneous inversion of hydrogeologic and thermal data 2: incorporation of thermal data. Water Resour Res 24(3):356–372

Ziagos JP, Blackwell DD (1986) A model for the transient temperature effects of horizontal fluid flow in geothermal systems. J Volcanol Geotherm Res 27(371):371–397